

## Research Article

# Prediction of Epidemic Transmission Path and Risk Management Method in Urban Subway

Xiaojun Xu , Sen Xiong , Yifeng Huang , and Rong Qin 

*School of Information and Management, Guangxi Medical University, Nanning, Guangxi 530021, China*

Correspondence should be addressed to Xiaojun Xu; [xuxiaojun@gxmu.edu.cn](mailto:xuxiaojun@gxmu.edu.cn)

Received 9 April 2022; Revised 9 May 2022; Accepted 16 May 2022; Published 31 May 2022

Academic Editor: Wen-Tsao Pan

Copyright © 2022 Xiaojun Xu et al. This is an open access article distributed under the Creative Commons Attribution License, which permits unrestricted use, distribution, and reproduction in any medium, provided the original work is properly cited.

With the development of COVID-19, the epidemic prevention requirements of city subway system have become stricter. This study studies the transmission path of epidemic disease in city subway system. Using FLUENT software and AnyLogic software, the simulation models of subway platform ventilation structure and crowd behavior mode in subway system are constructed, respectively, and SEIR (vulnerable exposed affected recovered) is used as the general infection model of epidemic disease. According to the actual situation, the parameters such as shoulder width, flow, and moving speed of crowd are determined, and the simulation analysis of epidemic disease transmission in subway system is carried out. The analysis results show that the transmission speed of the disease in the subway will increase with the enhancement of the transmission capacity of the disease and the increase of the contact rate. When the disease transmission capacity is 0.14, the number of latent persons reaches the peak at 14.115 time units, which is 1374, and the number of patients reaches the peak at 28.541 time units, which is 1925. According to the simulation results, the simulation analysis results show that with the enhancement of disease transmission ability and the increase of exposure rate, the maximum number of latent and sick people in the subway environment will increase. The corresponding suggestions on risk management and control of infectious disease transmission in subway are put forward. The research results can provide a useful reference for the epidemic prevention management of urban subway transportation system in China.

## 1. Introduction

Mankind has been threatened by infectious diseases since ancient times. After entering modern times, human methods to deal with infectious diseases have become more and more efficient, but they still cannot completely offset the damage caused by infectious diseases (Jabbar, 2020) [1]. As a relatively closed space, the subway system has smaller air flow degree than the outside world, dense personnel, fast personnel flow speed, and wide flow range. It is an ideal environment for the spread of infectious diseases (Su et al., 2020) [2]. If the prevention and control of infectious diseases in the urban subway system is not scientifically and reasonably prepared, the urban subway will become a major loophole in epidemic prevention during the epidemic period and pose a direct threat to the lives and lives of citizens (Mehra et al., 2020) [3].

The main method to study the transmission path and prevention and control mode of infectious diseases in urban

subway system is virtual simulation modeling. On the one hand, a representative subway platform space model in geometric characteristics is constructed according to the spatial size characteristics of real subway system, and the model is implemented by finite metadata simulation software FLUENT (Zhou et al., 2019) [4]. On the other hand, the research also models the behavior subject of the platform—passengers and their movement mode. Specifically, the research draws on the force concept of classical mechanics to design the traveler’s “social force” model, which accurately expresses the traveler’s movement mode in the subway system and gives the pedestrian’s shoulder width, moving speed, and other index values in the model with reference to the relevant data of pedestrians in reality. The simulation numerical analysis software AnyLogic designed by the concept of social force is used to build the pedestrian “social force” model (Fu et al., 2021) [5]. Shi et al. focused on the dynamics of malaria transmission based on time series data. A data-driven nonlinear stochastic model is proposed

to infer and predict the dynamics of malaria transmission according to the time series of epidemic data (Shi et al., 2020) [6]. The above three models are combined to analyze the spread of infectious diseases under the background of pedestrians moving in the subway system. According to the analysis of the transmission path law of infectious diseases in subway, some suggestions are put forward to optimize the development of epidemic prevention in urban subway (Cao et al., 2020) [7].

The innovation of this research lies in the following aspects. Firstly, the complex process of infectious disease transmission in the subway system is simplified to the disease transmission of each subway station and then combined with the actual spatial layout, geometric characteristics, ventilation, and other elements of the subway station. The simulation model of the subway platform is built by using the finite metadata simulation software FLUENT. Secondly, on the basis of understanding the pedestrian movement intention and referring to the force concept of classical mechanics, this paper creatively puts forward the “social force” model so as to more accurately describe the pedestrian movement law in the subway platform and set reasonable values for the parameters involved in the “social force” model one by one according to the actual situation of the subway system. For example, by counting the body height, shoulder width, and other data of adults, the elderly, young people, and children, the existence of pedestrians in the subway space model is simplified into a cylinder with the shoulder width of people of all ages as the diameter and the height of people of all ages as the height, which greatly simplifies the calculation method of the distance between pedestrians and obstacles in the subsequent “social power” model. The influence of the distance between pedestrians and other individuals or objects on their moving speed is quantified as a piecewise function. At the same time, we use the concept of “social force” proposed by Kozio et al. to carry out the numerical analysis of social force [8].

The full text can be divided into four parts. The first part is used to introduce the research background of the law of infectious disease transmission, the harm and control methods of infectious disease transmission in the subway, the technical methods and research ideas used in the research, the innovation of the full text, and so on. The main content of the second part is to establish the infection model of epidemic diseases in urban subway, including the design and simulation of subway station space model, pedestrian movement model, and general infection model of infectious diseases. The third part is used to analyze and present the calculation results of the simulation model and provide some constructive suggestions on subway epidemic prevention and control based on the analysis results. The fourth part is mainly used to summarize the content of the full text.

## 2. Related Works

Infectious diseases, especially those with obvious symptoms and high mortality, pose a great threat to mankind. Infectious disease experts and scholars all over the world have carried out a large number of relevant studies in order to

improve the ability of economies to prevent and control infectious diseases. Aimed at the spread of COVID-19 in Egypt, combined with the concept of partial derivative, an improved dynamic model for predicting COVID-19 propagation is established, and the prediction results are in good agreement with the actual report data (Raslan, 2021) [9]. Tiwari et al.’s research team designed a simple improved infectious disease transmission model based on SerD to study the transmission law of COVID-19 and predict the epidemic peak under the locking effect. The test results show that the epidemic peak predicted by the model is more accurate [10]. Considering the health insurance coverage and other factors in the study area, Fang et al. designed an infectious disease transmission model combined with machine learning method to predict the transmission peak of infectious diseases, and the simulation results show that the prediction performance of the model is good [11]. Fan et al. used the quasi-experimental analysis framework to analyze the situation of immigrants in Wuhan and COVID-19 data. It was found that the size of Wuhan immigrants was highly correlated with the number of confirmed cases per day. The results of this study help to monitor the epidemic prevention and control situation in various regions. Wan et al. proposed a new COVID-19 transmission dynamic model combined with the intervention measures implemented in China. The model was parameterized by Markov Chain Monte Carlo (MCMC) method to estimate the number of controlled propagation and effective daily reproduction rates of disease transmission in Chinese mainland (excluding Hubei). The estimated results show that the premature release of personal protection may prolong the transmission period of the disease, allow more people to be infected, and even lead to the second wave of epidemic or outbreak. Based on the assessment results, the research team suggested that in order to ensure that the epidemic is controlled at a reasonable level, it is necessary to maintain the current comprehensive restrictive interventions and self-protection measures, including travel restrictions, entry quarantine, contact tracking, and isolation and reduction of contact, such as wearing masks, maintaining social distance, and so on (Wan et al. 2020) [12].

Luo et al. applied long-term and short-term memory algorithm and extreme gradient enhancement algorithm to establish a daily confirmed case prediction model for the time series data of the number of infectious diseases in the United States and used MAE, MSE, RMSE, and MAPE to evaluate the fitting effect of the model. The results showed that isolating uninfected individuals to reduce the contact rate between susceptible individuals and infected individuals could effectively reduce the number of confirmed cases per day. Tyagi et al. have further explored all aspects of infectious diseases, combined with SEIQR (susceptible exposed infected quarantined recovered) mathematical model and long-term and short-term memory algorithm, designed an improved mathematical model to predict the infectious process of infectious diseases, and verified the model. The results show that the prediction result of the model is longer, and the short-term memory algorithm or SEIQR model is more accurate [13]. Mahajan et al.’s research team proposed

an epidemic model based on the epidemic law of Xinguan, which sets the disease transmission rate of symptomatic, asymptomatic, and exposed infected people to different values. The model is applied to the prediction of the number of COVID-19 infected persons in Germany and Korea. The results show that the prediction performance of the model is excellent [14]. Chaudhari et al. used a variety of machine learning algorithms to build a prediction model for the number of patients with new crowns in a specific region according to the existing data of patients with new crowns in major countries in the world, regional cleanliness, population number, population density, ambient temperature, environmental humidity, and other information and found that the prediction model based on linear regression was more effective [15].

To sum up, experts and scholars in the industry have put forward a large number of intelligent algorithms and models to predict the spread of infectious diseases, and some models have excellent prediction accuracy. However, there are few research data on the construction of special infectious disease transmission path prediction model for the specific scene of dense flow of people, that is, the subway transportation system. Therefore, based on the modeling of the physical environment and pedestrian behavior of the subway scene, this study attempts to build a simulation model to analyze the transmission path of infectious diseases in the subway so as to provide some references for improving the epidemic prevention ability of the urban subway scene.

### 3. Establishment of Epidemic Transmission Model of Urban Subway

*3.1. Simulation Design of Epidemic Prevention and Ventilation System of Urban Subway Platform Based on Fluent.* Tunnel ventilation or air conditioning system shall be set in the station hall and platform hall of subway station, section tunnel, turn back line, and end line tunnel. The equipment and management rooms in the station shall be equipped with local ventilation or local air conditioning system. The noise transmitted from the tunnel ventilation equipment to the station hall and platform hall shall not exceed 70 dB (a), and the noise transmitted to the ground air Pavilion shall meet the requirements of the current national environmental noise standards for urban areas. When the ventilation system of the station management room is sucked from the tunnel, the air inlet shall be set at the side of the train entering the station and the air outlet shall be set at the side of the train leaving the station. Urban rail transit is mostly built underground, lacking natural ventilation and light; coupled with the high population density on the rail transit line, the epidemic spreads more rapidly in this environment (Roy et al., 2020) [16]. Since the transmission direction and intensity of most infectious diseases are related to the ventilation of the environment, and the subway platform, as a key node in subway transportation, is very important to control the spread of the epidemic, it is necessary to analyze the ventilation environment of urban subway platform

(Wang et al., 2020) [17]. However, the constituent elements and changes of urban subway ventilation environment are complex, so its simulation analysis model needs to be established first to simplify the secondary influencing elements and components and highlight the core elements of ventilation environment (Paiva et al., 2020) [18].

At present, there are many subway stations using full-height semiclosed safety doors in China. Therefore, when establishing the ventilation environment model of subway platform, this form of safety door structure is selected as the basis (Feng et al., 2021) [19]. FLUENT is a common finite element numerical simulation software. Its simulation modeling process usually consists of the following steps: firstly, mesh the object's three-dimensional geometric model, then check the mesh division quality; then select the appropriate solution equation, define the attribute parameters of the model, and set the boundary conditions. The last step is to use FLUENT to calculate and iterate the model until the calculation results converge and output the required data and statistical charts. Sousa et al. estimated the number of cases within 80 days after the first case by solving the differential equation. The results are logarithmicized and compared with the actual values to observe the fitting of the model [20]. The air flow form in the subway platform can be simply regarded as turbulence. According to the mainstream simulation method of turbulence in the engineering field, the following formulas can be obtained.

$$\nabla \vec{u} = 0, \quad (1)$$

$$\frac{\partial u}{\partial t} + \nabla(u \vec{u}) = \frac{1}{\rho} \frac{\partial p}{\partial x} + \nu \nabla(\text{grad } u), \quad (2)$$

$$\frac{\partial v}{\partial t} + \nabla(v \vec{u}) = \frac{1}{\rho} \frac{\partial p}{\partial y} + \nu \nabla(\text{grad } v), \quad (3)$$

$$\frac{\partial w}{\partial t} + \nabla(w \vec{u}) = \frac{1}{\rho} \frac{\partial p}{\partial z} + \nu \nabla(\text{grad } w). \quad (4)$$

In (4),  $u$ ,  $v$ , and  $w$ , respectively, represent the velocity components of air velocity  $\vec{u}$  in all directions of three-dimensional coordinate space,  $\rho$  is the air density,  $p$  is the pressure value, and  $t$  represents time. Referring to the statistical average theory of turbulence, the instantaneous values of velocity and pressure can be decomposed into the combination of average value and pulsation value, as shown in the following equations.

$$u = \bar{u} + u', \quad (5)$$

$$v = \bar{v} + v', \quad (6)$$

$$w = \bar{w} + w', \quad (7)$$

$$p = \bar{p} + p'. \quad (8)$$

Moreover, the mean value of each variable in the time dimension can be expressed by

$$\bar{\phi} = \frac{1}{\Delta t} \int_t^{t-\Delta t} \phi(t) dt. \quad (9)$$

Combined with formulas (1)–(9), the continuity equation and momentum equation of turbulence can be obtained, as shown in the following equations, respectively.

$$\frac{\partial(\rho u_i)}{\partial x_i} = 0, \quad (10)$$

$$\frac{\partial}{\partial x_j}(\rho u_i u_j) = -\frac{\partial p}{\partial x_i} + \left( \mu \frac{\partial u_i}{\partial x_j} - \overline{\rho u_i' u_j'} \right). \quad (11)$$

Among them,  $x_j$  represents the position of subway platform  $j$  on the  $x$ -axis in the coordinate system,  $p$  is the pressure on turbulence,  $\mu$  is the viscosity coefficient of air, and  $\overline{\rho u_i' u_j'}$  is the Reynolds stress. The standard  $k - \varepsilon$  turbulence model is used to build the simulation space of this study, and its core calculation formula is shown as follows.

$$\begin{cases} \frac{\partial(\rho k u_i)}{\partial x_j} = \frac{\partial}{\partial x_j} \left[ \left( \mu + \frac{\mu_t}{\sigma_k} \right) \frac{\partial k}{\partial x_j} \right] + G_k + G_b - \rho \varepsilon - Y_M + S_k, \\ \frac{\partial(\rho \varepsilon u_i)}{\partial x_j} = \frac{\partial}{\partial x_j} \left[ \left( \mu + \frac{\mu_t}{\sigma_\varepsilon} \right) \frac{\partial \varepsilon}{\partial x_j} \right] + C_{1\varepsilon} \frac{\varepsilon}{k} (G_k + C_{3\varepsilon} G_b) - C_{2\varepsilon} \rho \frac{\varepsilon^2}{k} + S_\varepsilon, \end{cases} \quad (12)$$

where  $G_k$  and  $G_b$  represent the turbulent kinetic energy caused by velocity and buoyancy, respectively, and  $Y_M$  represents the increase of arterial expansion of the parameters generated by compressible turbulence.  $Y_M$  and  $Y_M$  are user-defined control parameters,  $C_{1g}$ ,  $C_{2g}$ , and  $C_{3g}$  represent empirical constants, and  $\sigma_k$  and  $\sigma_\varepsilon$  are Planck's coefficients corresponding to turbulent kinetic energy  $k$  and dissipation rate  $\varepsilon$ , respectively. When the air fluid is in a steady state, (12) can be simplified to

$$\begin{cases} \frac{\partial(\rho k u_i)}{\partial x_j} = \frac{\partial}{\partial x_j} \left[ \left( \mu + \frac{\mu_t}{\sigma_k} \right) \frac{\partial k}{\partial x_j} \right] + G_k - \rho \varepsilon, \\ \frac{\partial(\rho \varepsilon u_i)}{\partial x_j} = \frac{\partial}{\partial x_j} \left[ \left( \mu + \frac{\mu_t}{\sigma_\varepsilon} \right) \frac{\partial \varepsilon}{\partial x_j} \right] + C_{1\varepsilon} G_k \frac{\varepsilon}{k} - C_{2\varepsilon} \rho \frac{\varepsilon^2}{k}. \end{cases} \quad (13)$$

In addition, in formula (13),  $C_{1g} = 1.45$ ,  $C_{2g} = 1.90$ ,  $C_\mu = 0.09$ ,  $\sigma_\varepsilon = 1.30$ , and  $\sigma_k = 1.02$ . The above is the complete theoretical model of air flow in subway platform, and then use FLUENT software to build the geometric model of subway station according to this theoretical model. The subway station is designed as a cube with length, width, and height of 136 m, 11.5 m, and 3 m, respectively. The walls of the elevator and the subway station are simplified into smooth planes. The plan of the platform after the design is completed is shown in Figure 1.

Considering the geometric structure of the platform and the accuracy of simulation calculation, the platform structure is finally divided into 625711 networks and 729642 nodes by FLUENT software, and there is no grid with negative volume in the tested model. The decisive index of the model grid is calculated to be 0.87, which is greater than 0.3. It is considered that the grid quality is good and the division is reasonable.

In terms of model parameter setting, in the  $k - \varepsilon$  turbulence model, when entering and leaving the station, the wind speeds listed at different heights are also different. Combined with common sense, when setting the entering station, the wind speed at the position above 0.5 m is 1.2 m/s, the entering wind speed at the position above 0.5 m is 2.4 m/s, and the outgoing wind speed is fixed at 1.7 m/s (Mirza et al., 2020) [21].

**3.2. Establishment of Behavior Trajectory Simulation Model and Epidemic Disease Infection Model of Urban Subway Population.** The infection mode and law of subway epidemic also have obvious correlation with the movement track of passengers. The passenger volume of each city varies greatly in the order of magnitude, so it is difficult to visually compare the recovery of subway passenger volume among cities. Generally speaking, there is an uncertain bulk distribution of people in the subway. The greater the density of people, the more serious the spread of the epidemic. Therefore, it is necessary to model the movement route of passengers in the rail transit system. Here, AnyLogic software is selected to complete the modeling. Pedestrian movement patterns in the subway have intrinsic motivation, which must be taken into account when modeling their movement behavior (Wang et al., 2019) [22]. The so-called pedestrian intrinsic motivation behavior model refers to taking the subway station scene as the starting point of research. Assuming that the movement and state of passengers are continuous, the whole process of pedestrian activity in the station is analyzed. Thus, the law of pedestrians in the process of a series of continuous spatial displacement trajectories is analyzed so that relevant staff can accurately grasp the evolution process of station pedestrians under normal conditions. The influence of pedestrians' intrinsic motivation on their walking rules is summarized as "social force" (an artificially designed object based on the concept of classical mechanics). Specifically, the movement process of most pedestrians seeking to reach their destination as soon as possible in the subway system will be limited by various conditions of the surrounding environment, so the pedestrian self-drive can be expressed according to the following formula.

$$\vec{f}_a^0 = m_a \frac{\vec{v}_a^0 - \vec{v}_a}{\tau_a}. \quad (14)$$

Among them,  $\vec{f}_a^0$  represents the real-time self-driving force of passenger  $a$ , and  $m_a$ ,  $\tau_a$ ,  $\vec{v}_a^0$ , and  $\vec{v}_a$  represent the quality of pedestrian  $a$ , the time-consuming of adjusting behavior, the current expected movement speed, and the current actual movement speed, respectively. Pedestrians will also be affected by other people and environmental objects during walking. These effects are modeled and described below. The force  $\vec{f}_{ab}$  between pedestrians can be expressed by the following formula:

$$\vec{f}_{ab} = \vec{f}_{ab}^{ps} + \vec{f}_{ab}^{ph}. \quad (15)$$

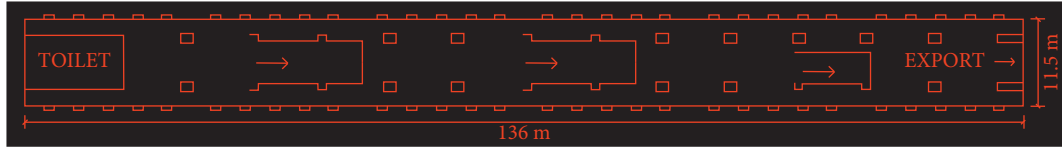


FIGURE 1: Plan structure of subway platform.

Among them,  $\vec{f}_{ab}^{ps}$  is the psychological force between pedestrians, which can be described according to formula  $\vec{f}_{ab}^{ps} = A \exp[d_{ab}/B] \cdot \alpha \cdot \vec{n}_{ab}$ .  $A$  and  $B$ , respectively, represent the force strength and force range between pedestrians,  $d_{ab}$  represents the distance between pedestrians,  $\vec{n}_{ab}$  is the force direction, and  $\alpha$  is the influence coefficient.  $\vec{f}_{ab}^{ph}$  is the physiological force between pedestrians, which can be described according to the formula  $\vec{f}_{ab}^{ph} = \mu \cdot (r_a + r_b - d) \cdot \vec{n}_{ab}$ .  $r_a$  and  $r_b$  represent the radius of the orthographic projection of the private space required by pedestrians under normal conditions.  $d$  is the straight-line distance between two people. When  $(r_a + r_b - d)$  is greater than 0, the distance between two people is not small enough to affect the movement of both sides. At this time, the repulsion coefficient should be taken as 0.

In addition to avoiding contact with other people's limbs, pedestrians also pay attention to avoiding obstacles in the environment. This action relationship can also be described in the form of force, expressed as  $\vec{f}^{\text{bar}} = k \cdot (r_a - d_{\text{bar}}) \cdot \vec{n}_a$ , where  $k$  is the repulsion force coefficient and  $d_{\text{bar}}$  is the distance between pedestrians and obstacles. Similarly, when  $(r_a - d_{\text{bar}})$  is greater than 0, it is considered that the distance between obstacles and pedestrians is too large to affect the latter's walking. At this time,  $k$  takes 0 and  $\vec{n}_a$  as the direction vector of the two forces.

AnyLogic software is developed on the basis of social force model, which is also the reason why it is selected for pedestrian trajectory modeling. The flow of pedestrian trajectory modeling of AnyLogic software is shown in Figure 2.

For example, the pedestrian modeling tools in godwall area are used to implement the pedestrian modeling tools in the godwall environment. Before behavior modeling, set the movement logic of pedestrians. According to the common sense of life, pedestrians first buy tickets and pass the security inspection, then choose the appropriate route to enter the station hall, and then enter the platform through the escalator or elevator. At this time, if they cannot get on the train for various reasons, continue to wait for the follow-up train; otherwise, they take the train. The above pedestrian behavior logic can be realized through PedGoTo, PedService, and other controls in AnyLogic pedestrian library. Since the model cannot simulate all the details of passengers entering the platform, certain assumptions and simplification are required (Xiong et al., 2019) [23]. According to the geometric dimension data of human body, the orthographic projection shape of pedestrian on the ground is simplified into a circle, and the diameter is taken as the random value within the range of 0.4 m~0.5 m of adult shoulder width. The

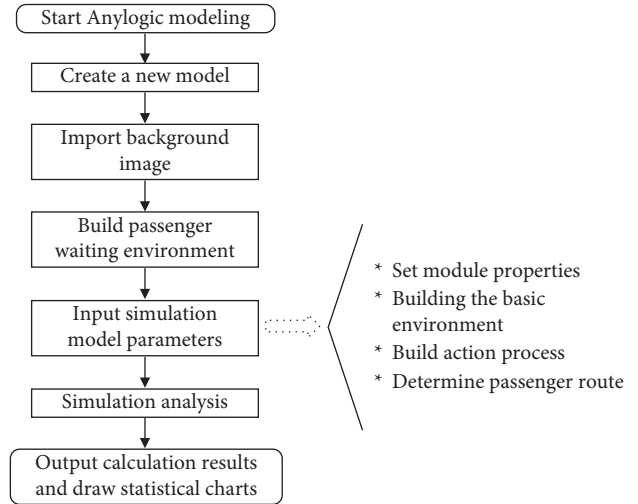


FIGURE 2: Pedestrian trajectory modeling process of AnyLogic software.

traveling speed is determined as 1.32 m/s. The average hourly inflow and outflow of subway stations are 1300 and 1600 according to the average level of domestic subway.

Since the train is set to start at an interval of 6 minutes, passengers getting off the train are also set to take the door as the source, generate it every 6 minutes, and exit the station through the nearest elevator. Finally, according to the general mode of infectious disease transmission in the model, the more mature SEIR model is selected.

#### 4. Simulation Analysis of Urban Subway Epidemic Spread

In this paper, the simulation models of subway platform ventilation structure and crowd behavior mode of subway system are established by using FLUENT software and AnyLogic software, and SEIR is taken as the general infection model of epidemic. By simultaneous interpretation of the number of people in the SEIR model over time, we will lay a foundation for the analysis of the number of people who are most affected by the infection and the number of the sick people.

First, simultaneously interpreting the spread of disease under different transmission capacity, the basic reproductive number of infectious diseases must be greater than 1; otherwise, infectious diseases cannot spread in the computational space, as shown in Figure 3.

*Figure 3 Simulation Statistics.* The initial number of patients is set according to 10% of the number of people in the subway at the same time, that is, 290 people. It can be

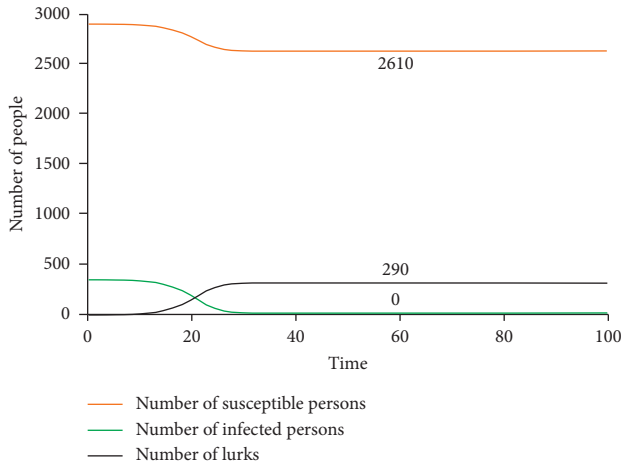


FIGURE 3: Changes in the number of different types of people over time when the basic regeneration number is 0.01.

seen that when the basic regeneration number is less than 1, the transmission speed of the disease in the subway population is lower than the flow speed of the population and the recovery speed of the disease. Therefore, in this case, the disease cannot spread in the subway space, so the basic regeneration number index must be set to a value greater than 1 to carry out subsequent research. Referring to the relevant data of infectious disease research, the contact rate of latent persons is 8.781, the basic regeneration number index is set to 5, the duration of infectious diseases is 53.214 time units, the incubation period is 6.302 time units, and the transmission capacity is set to 0.08. The change curve of various populations over time calculated by substituting into the simulation model is shown in Figure 4.

According to the analysis of Figure 4, when the simulation time is 100 time units, the number of latent persons reaches the maximum value of 1043 in the 30th minute, and the number of patients reaches the maximum of 2086 in the 44th minute. According to the data in Figure 3, the change step of follow-up propagation ability ( $I$ ) index should be 0.03, and the selected values are 0.02, 0.05, 0.08, 0.11, and 0.14. Run the simulation model according to these five values to obtain the latent real-time curve cluster and the sick real-time curve cluster, which are shown in Figure 5 and 6, respectively.

It can be seen from Figure 5 that with the enhancement of disease transmission capacity, the time taken for the number of disease latent persons to reach the peak is gradually shortened, and the peak number increases significantly. When the disease transmission capacity is 0.14, the number of latent persons reaches the peak at 14.115 time units, which is 1374. Reanalyze the real-time curve of patients, as shown in Figure 6.

It can be seen from Figure 6 that with the enhancement of disease transmission ability, the real-time curve of the sick population shows the same change trend as the real-time curve of the latent, with the peak increasing and the peak time shortening. When the transmission capacity is 0.14, the number of patients reaches the peak at 28.541 time units, which is 1925.

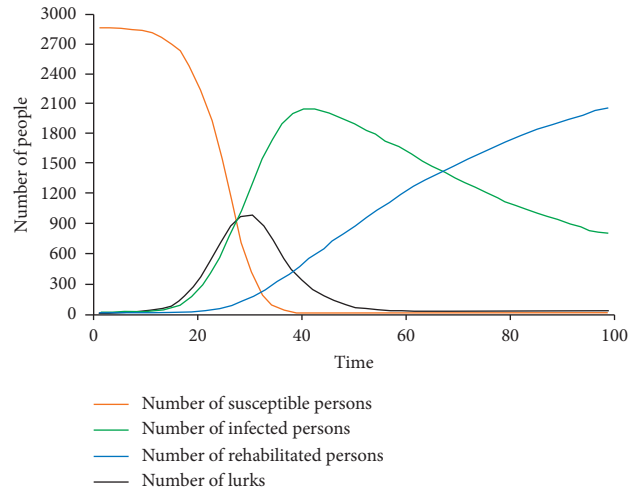


FIGURE 4: Changes of the number of different types of people over time when the transmission capacity is 0.08.

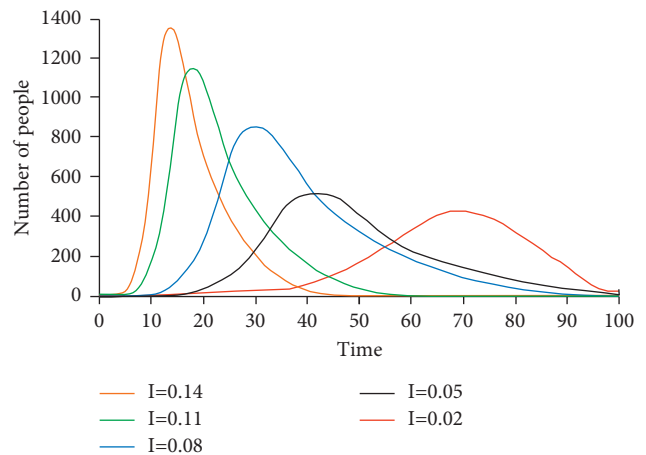


FIGURE 5: Real-time curve of latent persons under various infectious disease transmission capacity parameters.

Then, analyze the spread of the disease under different contact rates. The core parameters of the disease are set as follows: the transmission capacity is fixed at 0.116, the disease duration is 52.174 time units, the incubation period is 6.402 time units, and the contact rate ( $CR$ ) is 15.0. The time-varying curves of various populations calculated by substituting various parameters into the simulation model are shown in Figure 7.

It can be seen from Figure 7 that when the simulation time is 100 time units, the number of latent persons reaches the maximum value of 1285 in the 19th minute, and the maximum number of patients reaches 2120 in the 32nd minute. According to the data in Figure 6, the  $CR$  change step of the disease in the follow-up analysis should be 3, and the selected values are 3.0, 6.0, 9.0, 12.0, and 15.0. Run the simulation model according to these five values to obtain the latent real-time curve cluster and the sick real-time curve cluster, which are shown in Figures 8 and 9, respectively.

As shown in Figure 8, with the increase of the contact rate of infectious diseases in the subway space, the time for

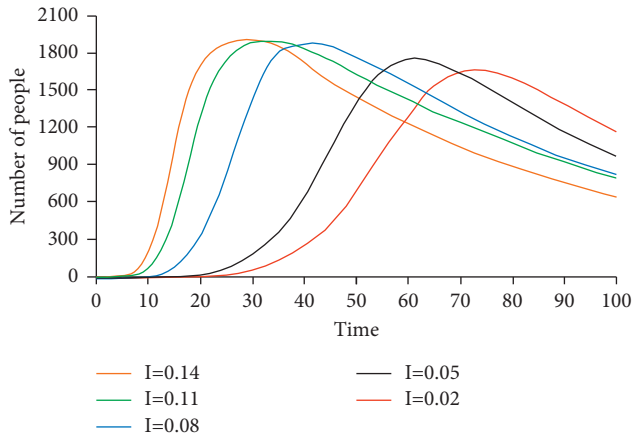


FIGURE 6: Real-time curve of patients under various infectious disease transmission capacity parameters.

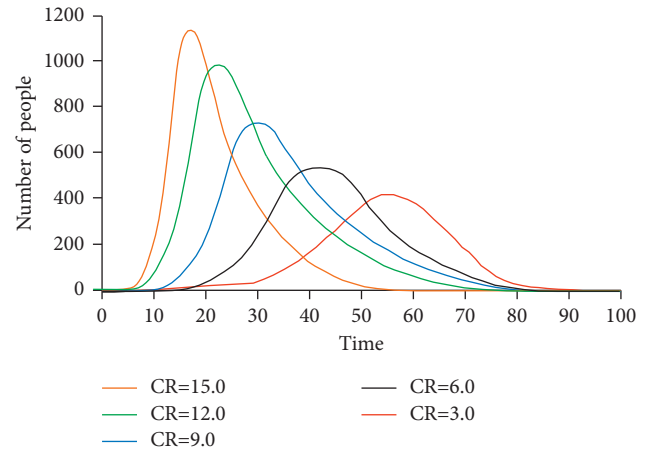


FIGURE 8: Real-time curve of latent persons under various infectious diseases' exposure rate parameters.

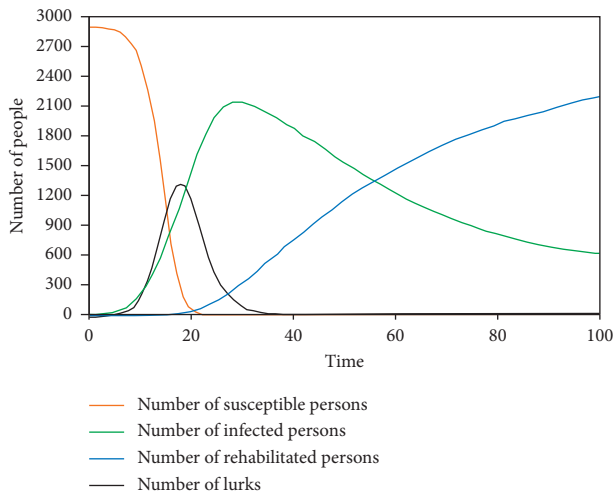


FIGURE 7: Changes in the number of different types of people over time when the exposure rate is 15.0.

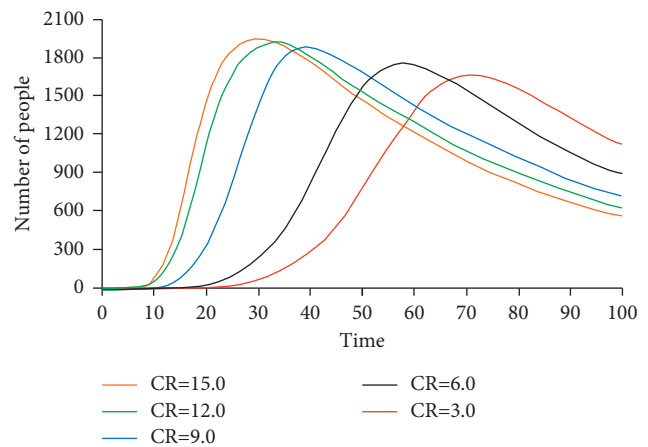


FIGURE 9: Real-time curve of patients under exposure rate parameters of infectious diseases.

the number of disease latent persons to reach the peak is gradually shortened, and the peak number increases significantly, which is roughly the same as that in Figure 5. When the propagation rate is 15.0, the number of lurks reaches a peak of 1154 at 16.362 time units. Reanalyze the real-time curve cluster of patients, as shown in Figure 9.

It can be seen from Figure 9 that with the increase of the contact rate of infectious diseases in the subway space, the maximum number of patients becomes larger and larger, and the time to reach the maximum becomes shorter and shorter. When the transmission rate was 15.0, the number of patients reached the peak at 31.27 time units, which was 19.69.

Combined with the above analysis, the transmission speed of infectious diseases will be greatly affected by the transmission capacity and contact rate. Therefore, the priority path for the transmission of infectious diseases is in the most densely populated subway entrances, elevators, stairs, and places that are more suitable for virus transmission, such as ambient temperature, humidity, and ventilation. In this regard, this study puts forward the following suggestions on

the risk control of subway epidemic disease transmission (the proposed assumption is that there have been infectious disease cases in the city where the subway is located) [24]. First, people in the subway system should wear masks and keep a certain distance from others as far as possible to reduce the potential transmission efficiency of the disease. Second, the subway system space in high-risk areas should be regularly disinfected and tested for viruses in the environment so as to minimize the potential source of infection. Finally, the subway should reasonably arrange pedestrian flow guidance signs and guides to evacuate the dense subway pedestrian flow as far as possible so as to reduce the contact rate of pedestrians in the environment. If the epidemic prevention pressure around the subway is high, the facilities with high pedestrian density in areas such as elevators can be limited or stopped directly.

### 5. Conclusion

In order to explore the transmission path of the epidemic disease in the urban subway system, the simulation models of subway platform ventilation structure and crowd

behavior mode in the subway system were constructed by using FLUENT software and AnyLogic software, and SEIR was used as the general infection model of the epidemic disease. The simulation analysis results show that the maximum number of latent and sick people in the subway environment will increase with the enhancement of disease transmission ability and the increase of contact rate. Specifically, when the disease transmission ability is 0.14, the number of latent people reaches the peak at 14.115 time units, 1374 people, and the number of sick people reaches the peak at 28.541 time units, 1925 people. When the transmission rate was 15.0, the number of latent persons peaked at 16.362 time units, 1154, and the number of sick persons peaked at 31.27 time units, 1969. Therefore, the most densely populated subway entrances, elevators, stairs, ambient temperature, humidity, ventilation, and other factors are more suitable for virus transmission, which is the priority path of infectious disease transmission. Based on the research results, the following suggestions are put forward to ensure that pedestrians in the subway system of cities with cases should wear masks and keep a distance; regularly disinfect the environment; and evacuate the relatively densely populated areas in the subway. However, providing more convenience in the subway scene is a hot issue in the current industry. With the complexity of the evolution of large subway passenger flow, it has become the research direction of the industry to reproduce the subway passenger flow organization in the form of "optimization model." This paper does not carry out the simulation research of subway large passenger flow based on multilevel pedestrian behavior model to analyze the maximum evacuation capacity of different facilities. Therefore, it needs to be studied to realize the effective regulation of large passenger flow organization [24, 25].

### Data Availability

The data used to support the findings of this study are available from the corresponding author upon request.

### Conflicts of Interest

The authors declare that they have no known competing financial interests or personal relationships that could have appeared to influence the work reported in this paper.

### Acknowledgments

This work was supported by Guangxi Health and Economic and Social Development Research Center in 2021: Research on Network Public Opinion Dissemination Mechanism and Early Warning of Public Health Emergencies (no. 2021RWB19), and Key Textbook Construction Project of Guangxi Medical University in 2021: Public Health Crisis Public Opinion Dissemination and Early Warning (no. Gxmuzdjc2118).

### References

[1] A. H. Jabbar, "Modeling of epidemic transmission and predicting the spread of infectious disease," *Systematic Reviews in Pharmacy*, vol. 11, no. 6, pp. 188–195, 2020.

[2] L. Su, N. Hong, X. Zhou, and J. Y. H. L. F. G. W. Y. He, "Evaluation of the secondary transmission pattern and epidemic prediction of COVID-19 in the four metropolitan areas of China," *Frontiers of Medicine*, vol. 7, no. 7, 171 pages, 2020.

[3] A. H. Amiri Mehra, M. Shafieirad, Z. Abbasi, and I. Zamani, "Parameter estimation and prediction of COVID-19 epidemic turning point and ending time of a case study on SIR/SQAIR epidemic models," *Computational and Mathematical Methods in Medicine*, vol. 2020, no. 4, pp. 1–13, 2020.

[4] G. Zhou, J.-Y. Jiang, C. J. T. Ju, and W. Wang, "Prediction of microbial communities for urban metagenomics using neural network approach," *Human Genomics*, vol. 13, no. S1, pp. 47–59, 2019.

[5] S. Fu, Y. Xiong, and L. Yi, "COVID-19 epidemic prediction model and prevention and control analysis," *Journal of Physics: Conference Series*, vol. 1992, no. 4, pp. 1–7, 2021.

[6] B. Shi, S. Lin, Q. Tan et al., "Inference and prediction of malaria transmission dynamics using time series data," *Infectious diseases of poverty*, vol. 9, no. 1, pp. 95–13, 2020.

[7] S. Cao, P. Feng, and P. Shi, "Application of modified SEIR epidemic dynamic model in prediction and evaluation of COVID-19 in Hubei," *Zhejiang da xue xue bao. Yi xue ban = Journal of Zhejiang University. Medical sciences*, vol. 49, no. 2, pp. 178–184, 2020.

[8] K. Koziol, R. Stanisawski, and G. Bialic, "Fractional-order SIR epidemic model for transmission prediction of COVID-19 disease," *Applied Sciences*, vol. 10, no. 23, pp. 1–9, 2020.

[9] W. E. Raslan, "Fractional mathematical modeling for epidemic prediction of COVID-19 in Egypt," *Ain Shams Engineering Journal*, vol. 12, no. 3, pp. 3057–3062, 2021.

[10] V. Tiwari, N. Deyal, and N. S. Bisht, "Mathematical modeling based study and prediction of COVID-19 epidemic dissemination under the impact of lockdown in India," *Frontiers in Physics*, vol. 8, no. 11, pp. 1–8, 2020.

[11] W. Fang, Y. Wang, and Z. Lu, "Prediction of an epidemic with machine learning and covid-19 data," *E3S Web of Conferences*, vol. 245, no. 1, pp. 1–5, 2021.

[12] H. Wan, J.-A. Cui, and G.-J. Yang, "Risk estimation and prediction of the transmission of coronavirus disease-2019 (COVID-19) in the mainland of China excluding Hubei province," *Infectious Diseases of Poverty*, vol. 9, no. 1, pp. 116–119, 2020.

[13] S. Tyagi, S. Gupta, S. Abbas, and K. P. B. Das, "Analysis of infectious disease transmission and prediction through SEIQR epidemic model," *Nonautonomous Dynamical Systems*, vol. 8, no. 1, pp. 75–86, 2021.

[14] A. Mahajan, N. A. Sivadas, and R. Solanki, "An epidemic model SIPHERD and its application for prediction of the spread of COVID-19 infection in India," *Chaos, Solitons & Fractals*, vol. 140, no. 11, 6 pages, Article ID 110156, 2020.

[15] A. N. Desai, M. U. G. Kraemer, and S. Bhatia, "Real-time epidemic forecasting: challenges and opportunities," *Health Security*, vol. 17, no. 4, pp. 268–275, 2019.

[16] "Spatial prediction of COVID-19 epidemic using ARIMA techniques in India," *Modeling Earth Systems and Environment*, vol. 7, no. 2, pp. 1385–1391, 2020.

[17] H. Wang, K. Xu, Z. Li, K. Pang, and H. He, "Improved epidemic dynamics model and its prediction for COVID-19 in Italy," *Applied Sciences*, vol. 10, no. 14, pp. 1–11, 2020.

[18] H. M. Paiva, R. J. M. Afonso, I. L. de Oliveira, and G. F. Garcia, "A data-driven model to describe and forecast the dynamics of COVID-19 transmission," *PLoS One*, vol. 15, no. 7, Article ID e0236386, 2020.



- [19] S. Feng, Z. Feng, C. Ling, C. Chang, and Z. Feng, "Prediction of the COVID-19 epidemic trends based on SEIR and AI models," *PLoS One*, vol. 16, no. 1, Article ID e0245101, 2021.
- [20] G. J. B. Sousa, T. S. Garces, V. R. F. Cestari, T. M. M. Moreira, R. S. Florêncio, and M. L. D. Pereira, "Estimation and prediction of COVID-19 cases in Brazilian metropolises," *Revista Latino-Americana de Enfermagem*, vol. 28, no. e3345, 8 pages, Article ID e3345, 2020.
- [21] T. Mirza, M. M. Hassan, and M. W. Hussain, "Prediction of COVID-19 trend in India using time series forecasting," *Indian Journal of Science and Technology*, vol. 13, no. 32, pp. 3248–3274, 2020.
- [22] L. Wang, C. Liang, W. Wu, and S. J. X. Y. C. Wu, "Epidemic situation of brucellosis in jinzhou city of China and prediction using the ARIMA model," *The Canadian Journal of Infectious Diseases & Medical Microbiology*, vol. 2019, no. 6, 9 pages, Article ID 1429462, 2019.
- [23] Z. Xiong, J. Zheng, D. Song, and S. Q. Zhong, "Passenger flow prediction of urban rail transit based on deep learning methods," *Smart Cities*, vol. 2, no. 3, pp. 371–387, 2019.
- [24] C. Fan, L. Liu, W. Guo, and A. C. M. M. P. H. Y. Yang, "Prediction of epidemic spread of the 2019 novel coronavirus driven by spring festival transportation in China: a population-based study," *International Journal of Environmental Research and Public Health*, vol. 17, no. 5, 1679 pages, 2020.
- [25] J. Luo, Z. Zhang, Y. Fu, and F. Rao, "Time series prediction of COVID-19 transmission in America using LSTM and XGBoost algorithms," *Results in Physics*, vol. 6, no. 3, pp. 1–9, 2021.